Environmental Pollution xxx (2016) 1–9

Contents lists available at ScienceDirect

Environmental Pollution

journal homepage: www.elsevier.com/locate/envpol

Metal enrichment and lead isotope analysis for source apportionment in the urban dust and rural surface soil☆

Yang Yu [a, b], Yingxia Li [a, *], Ben Li [b], Zhenyao Shen [a], Michael K. Stenstrom [b]

[a] State Key Laboratory of Water Environment Simulation, School of Environment, Beijing Normal University, Beijing, 100875, China
[b] Department of Civil and Environmental Engineering, University of California Los Angeles, Los Angeles, CA, 90095, USA

ARTICLE INFO

Article history:
Received 28 March 2016
Received in revised form
12 June 2016
Accepted 21 June 2016
Available online xxx

Keywords:
Urban dust
Rural surface soil
Metal
Pb isotope
Beijing

ABSTRACT

To understand the metal accumulation in the environment and identify its sources, 29 different metal contents and lead (Pb) isotope ratios were determined for 40 urban dust samples, 36 surface soil samples, and one river sediment sample collected in the municipality of Beijing, China. Results showed that cadmium, copper (Cu), mercury, Pb, antimony (Sb), and zinc demonstrated to be the typical urban contaminants and mostly influenced by the adjacent human activities with higher content to background ratios and SD values. Among the 29 metal elements investigated, Cu and Sb were found to be the most distinct elements that were highly affected by the developing level and congestion status of the cities with much higher contents in dust in more developed and congested cities. There was a relatively wider range of Pb isotope ratios of country surface soil than those of urban dust. The results of source identification based on Pb isotope ratios showed that coal combustion was the first largest Pb source and vehicle exhaust was the second largest source. The sum of them accounted for 74.6% mass proportion of overall Pb pollution on average. The surface soil sample collected at an iron mine had the highest $^{204}Pb/^{206}Pb$, $^{207}Pb/^{206}Pb$, and $^{208}Pb/^{206}Pb$ ratios indicating ore had much higher ratios than other sources. The fine particle subsamples had higher $^{204}Pb/^{206}Pb$, $^{207}Pb/^{206}Pb$, and $^{208}Pb/^{206}Pb$ ratios than the coarse particle subsamples indicating more anthropogenic sources of coal combustion and vehicle exhaust for fine particles and more background influence for coarse particles. These results help with pinpointing the major Pb sources and applying suitable measures for the target sources.

1. Introduction

Urban dust and rural surface soils are good indictors of the accumulation of metal contamination from human activities (Sezgin et al., 2004; Christoforidis and Stamatis, 2009; Acosta et al., 2015; Song et al., 2015). Both are mobile and can be easily suspended by wind or transported in stormwater runoff (Davis et al., 2001; Lau et al., 2009; Egodawatta et al., 2013). High metal contents are often found in environmental media because of the rapid industrialization and urbanization (Li et al., 2013; Lu et al., 2014; Madarang and Kang, 2014). Human exposure to metal pollutants in urban dust and rural surface soil through inhalation, direct ingestion, and dermal contact can adversely affect human health (Granero and Domingo, 2002). Most metals will harm human internal organs if the safe dose levels are exceeded but this is especially the case for some toxic metals such as lead (Pb), chromium (Cr), and cadmium (Cd), which are often known as "chemical time bombs" (Stigliani et al., 1991). Tracing the sources of heavy metals in urban dust and rural surface soil is of key importance for our understanding of their behavior and to control the exposure risk (Žibret, 2012).

Sources of various metals in urban environments are numerous and often difficult to identify. Statistical analyses, such as principal component analysis, clustering analysis, and multivariate statistical analysis, were popularly used to identify the sources and pathways of heavy metal contamination (Franco-Uría et al., 2009; Lu et al., 2010; Zhao and Li, 2013). These methods are easy to use, but usually provide only general information on the sources. Isotopic fingerprinting, which is based on the ratios of stable isotopes, is a more in-depth method used to identify the origins of various contaminants (Diaz-Somoano et al., 2009; Gao et al., 2013). Stable isotopes of carbon, oxygen, Pb, and other metals have frequently been used to identify the sources.

☆ This paper has been recommended for acceptance by W. Wen-Xiong.

* Corresponding author.
E-mail address: yingxia@bnu.edu.cn (Y. Li).

http://dx.doi.org/10.1016/j.envpol.2016.06.046
0269-7491/

There are four naturally occurring Pb stable isotopes (^{204}Pb, ^{206}Pb, ^{207}Pb, ^{208}Pb). Their abundance extensively varies because of different decay pathways from ^{238}U, ^{235}U and ^{232}Th to ^{206}Pb, ^{207}Pb, ^{208}Pb, respectively (Faure, 1986). Different types of ore deposits and anthropogenic sources have their distinct isotopic ratios or signatures (Cheng and Hu, 2010). The Pb isotope ratio did not change in industrial or environmental processing, and retained its characteristic ratio from its source ore (Ault et al., 1970). The Pb isotope ratios can be used to identify the sources and transport pathways of Pb in pollution studies (Hu et al., 2014; Liu et al., 2014; Han et al., 2015).

Certain studies have shown that the qualitative analysis based on the Pb isotope ratios have been well performed in many study areas (Zhu et al., 2013; Hu et al., 2014, 2015a). The Pb isotope ratios were determined for various environmental media including organisms, atmospheric aerosol, soil, urban dust, sediment and so on (Ip et al., 2005; Widory et al., 2010; Zhu et al., 2013; Hu et al., 2015b). At the same time, the Pb isotope ratios of pollution sources were also investigated such as coal combustion, mining, industrial emissions, vehicle exhaust (Bi et al., 2013; Liu et al., 2014; Hu et al., 2014). Normally Pb isotope was used to pinpoint the sources of Pb poisoning based on comparing the Pb isotope ratios of samples with those of possible sources. For quantitative calculation, more work should be done to promote this method.

The objectives of this study are (1) to analyze the contents of 29 different metals and their spatial distributions in urban dust and rural surface soil; (2) to characterize the Pb isotope ratios of urban dust and rural surface soil from different development areas; (3) to calculate the contribution from different Pb-related sources through Pb isotope ratios. The research results are expected to help environmental scientists and regulators to better understand the behavior of metals in soils and dusts of different developing areas and to manage the human and environmental exposure risks.

2. Materials and methods

2.1. Study sites

The municipality of Beijing is a typically well-developed region in northern China, which includes six central urban districts and ten developing districts with 142 towns and large county areas (Beijing Statistics Bureau, 2013). Fig. 1 shows the three sampling areas with 77 sampling sites representing different development status of the municipality of Beijing: Beijing center (BJC, central urban) located in the central urban districts, Miyun Town (MYT, town) in the developing districts, and Miyun County (MYC, rural county) located in the rural area of the developing districts. The BJC is a densely populated area with a population density of 8972 persons/km^2, while MYT is a small town that is less densely populated and MYC is a rural area composed primarily of agricultural land, grasslands, and mountains with a population density of 213 persons/km^2 (Beijing Statistics Bureau, 2013). Overall, 40 surface dust and 36 surface soil samples were collected from urban area (BJC and MYT) and rural area (MYC), respectively, as the representative media containing typical pollution from human activities in different developing level areas. Considering surface soils and dust could contribute particle matter and pollutants to the hydrosphere when it rains, one sediment sample was collected to compare with surface dust and soil samples.

2.2. Sampling

A total of 30 urban dust samples were collected from BJC in September and October 2012; a total of 10 urban dust samples were collected in MYT in January 2013; a total of 36 surface soil samples were collected from Sites 1 to 36 in December 2012 over the entire MYC area. In addition, one surface sediment sample was collected from Site 37 in the Baihe River in December 2012. Detailed information about the sampling sites is contained in Supplementary Table S1.

The sampling method for the urban dust and rural surface soil was described in our previous study (Li et al., 2016). Subsamples taken from Sites 14 and 28 in BJC were sieved through a 120 μm opening nylon sieve to produce large and small fractions (BJC14a: particle diameter > 120 μm, BJC14b: particle diameter < 120 μm; BJC28a: particle diameter > 120 μm and BJC28b: particle diameter < 120 μm). These fractions were used to analyze the difference in metal contents between different particle sizes.

One surface sediment sample was collected in December 2012 from Site 37 in the Baihe River, which was upstream of the Miyun Reservoir. The surface sediment sample was collected from the river bottom using a stainless steel shovel and deposited into a self-sealing plastic bag. The surface sediment sample was air dried for one month and extraneous matter such as leaves and large stones were removed.

2.3. Analysis of metal contents

All air-dried dust, soil, and sediment samples (including the subsamples of BJC14 and BJC28) were ground into particles less than 200 μm in diameter and stored at 4 °C before analysis. Approximately 0.5 g of the ground sample powder was digested using hydrofluoric acid, nitric acid, perchloric acid and aqua regia according to the national standard method for China (GB, 1995). Then the contents of Cd, cerium (Ce), cobalt (Co), copper (Cu), lanthanum (La), molybdenum (Mo), niobium (Nb), neodymium (Nd), nickel (Ni), Pb, scandium (Sc), thallium (Tl), yttrium (Y), and zinc (Zn) were determined by inductively coupled plasma-mass spectrometry (ICP-MS). In addition, the contents of barium (Ba), Cr, manganese (Mn), rubidium (Rb), strontium (Sr), titanium (Ti), aluminium (Al), ferric (Fe), magnesium (Mg), calcium (Ca), sodium (Na), and kalium (K) were determined by inductively coupled plasma-optical emission spectrometer (ICP-OES). In order to get the contents of arsenic (As), antimony (Sb) and mercury (Hg), aqua regia, potassium permanganate and oxalate were used to digest the ground sample powder. Then As and Sb contents were determined using hydride generation-atomic fluorescence spectrometry (HG-AFS). The content of Hg was determined using cold vapor generation-atomic fluorescence spectrometry (CV-AFS).

The limits of detection for As, Ce, Co, Cu, La, Sc, and Y were 1 μg/g. The limits of detection for Nb, Ni, Pb, and Zn was 2 μg/g. The limits of detection for Ba, Cr, Rb, and Sr were 5 μg/g. The limits of detection for Mn, Ti, Mo, Tl, Sb, and Cd were 10, 10, 0.2, 0.1, 0.05, and 0.02 μg/g, respectively. The limit of detection for Hg was 2 ng/g. The limits of detection for Al and Fe were 0.1% and the detection limit for Mg, Ca, Na, and K was 0.05%, respectively. Duplicate samples (one duplicate every 10 samples) were measured for data quality assurance. The recovery rate was obtained from adding geochemical reference materials (e.g., GSS17, GSS25, GSS26, and GSS27) (one every 10 samples) and calculated to be the ratio of the determined value and reference value of the reference material. The recovery rate ranged from 80.3% to 122.4%.

2.4. Pb isotope analysis

A total of 38 dust samples from BJC and MYT, excluding BJC14 and BJC28, were chosen for Pb isotope analysis. The Pb isotopes of the four subsamples BJC14a, BJC14b, BJC28a, and BJC28b were also analyzed. For MYC, we analyzed a total of 20 soil samples and one sediment sample. Locations of the Pb isotope analyses are shown

Please cite this article in press as: Yu, Y., et al., Metal enrichment and lead isotope analysis for source apportionment in the urban dust and rural surface soil, Environmental Pollution (2016), http://dx.doi.org/10.1016/j.envpol.2016.06.046

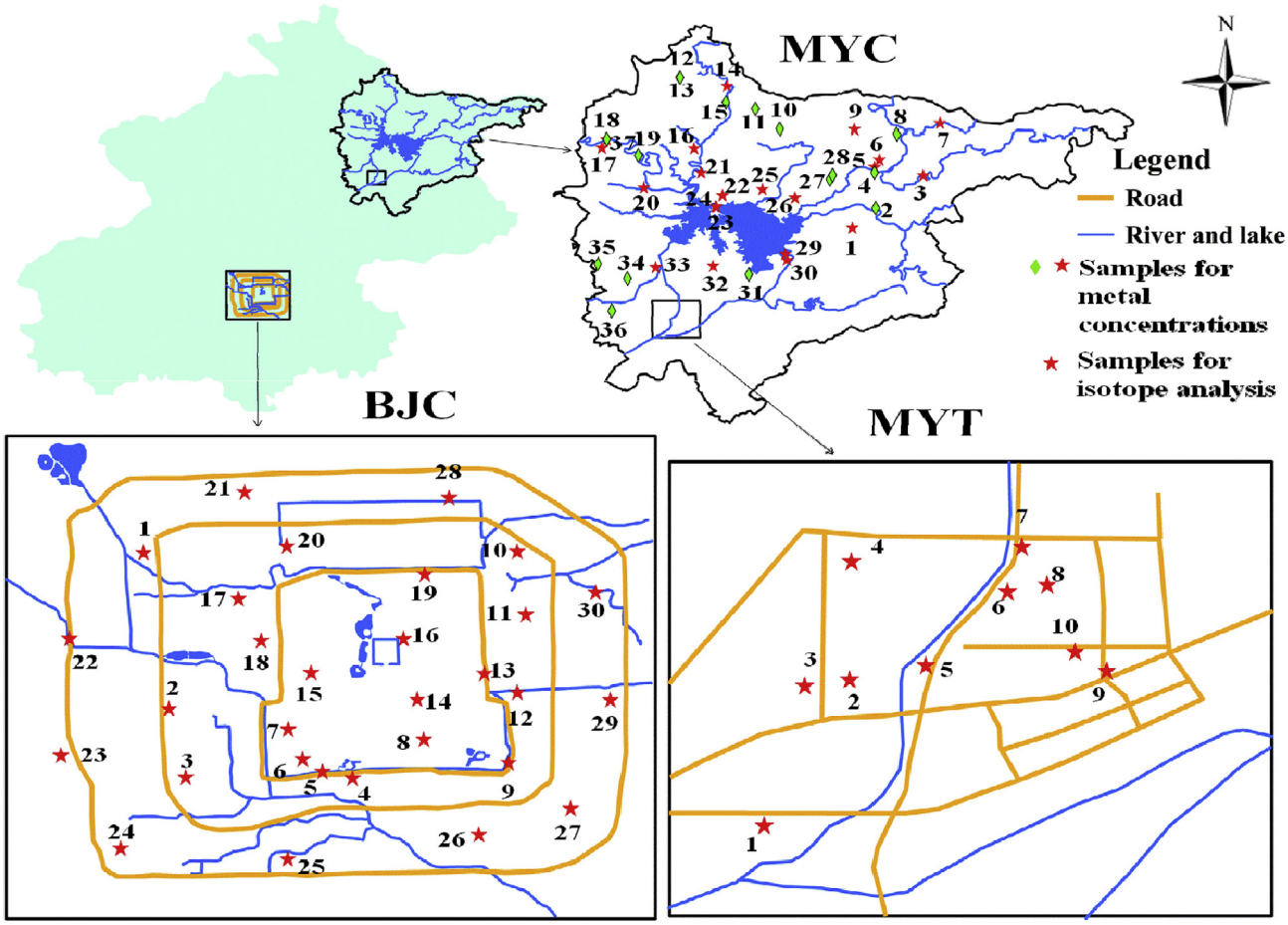

Fig. 1. Sampling locations in Beijing center (BJC), Miyun Town (MYT), and Miyun County (MYC), China.

with red stars in Fig. 1.

The air-dried dust, soil, and sediment samples were ground into particles less than 74 μm particle diameter (200 mesh). The samples were then heated at 550 °C for half an hour in a muffle furnace to destroy the organic matter in the samples. The samples were sequentially digested with HNO_3–HF–HCl–HBr in a Teflon beaker. The extracted samples were purified and then $^{206}Pb/^{204}Pb$, $^{207}Pb/^{204}Pb$, $^{208}Pb/^{204}Pb$, $^{208}Pb/^{206}Pb$, and $^{207}Pb/^{206}Pb$ analyses were carried out on a MicroMass Isoprobe multi-collector inductively coupled plasma mass spectrometer at the Guangzhou Institute of Geochemistry, Chinese Academy of Sciences. Every sample test consisted of 100 cycles and the mean value of 100 cycles was used as the isotope value.

Thallium as an internal control was used to correct Pb mass fractionation, which greatly improved the reproducibility of the isotope analysis. The Pb isotopic ratios reported in this work were corrected using standard reference material (SRM981, National Institute of Standards and Technology, NIST, USA). The NIST SRM 981 was run after every five samples separately to compensate for any mass bias and to assess precision. BCR-2 and JB-3, reference materials from the United States Geological Survey (USGS) and Geological Survey of Japan (GSJ), respectively, were measured with the samples to examine Pb isotope experimental process accuracy. The results of BCR-2 and JB-3 were all within the reference range, which demonstrated little Pb pollution during the experimental process. Pb isotope ratio results were reliable.

2.5. Data analysis

Descriptive statistical analyses were performed by the Microsoft Excel 2010, Matlab R2010b ArcGIS 10.0, Origin 8.0 and SPSS19.0. Fig. 1 and Fig.3 were drawn through ArcGIS 10.0. Fig. 2 and Fig. 4 were performed by Origin 8.0.

Inverse distance weighting (IDW) is an interpolation method widely applied to elucidate spatial distribution of many parameters. IDW assumes that the predictions are a linear combination of available data, which are weighted according to their distance from the point of being interpolated. Studies showed that distribution of metal elements had similar characteristics to IDW's assumption (Gu et al., 2012), IDW interpolation with power of 2 and the neighboring samples of 12 was applied to visualize the spatial distribution of metal contents in urban dust and rural surface soil using ArcGIS 10.0.

3. Results and discussion

3.1. Metal enrichment in urban dust and rural surface soil

The descriptive statistics of the 29 metal elements in the 76 samples from the three study areas, together with the background values, are shown in Table 1. Metal contents had a large range from 0.02 μg/g (Hg in MYC) to 11,067 μg/g (Ti in MYC) owing to the various enrichments in the natural environment and the different emission intensities from human activities. Standard deviation (SD) values of Cd, Cu, Hg, Mo, Pb, Sb, and Zn are more than half of the

Please cite this article in press as: Yu, Y., et al., Metal enrichment and lead isotope analysis for source apportionment in the urban dust and rural surface soil, Environmental Pollution (2016), http://dx.doi.org/10.1016/j.envpol.2016.06.046

Table 1
Descriptive statistics of metal contents in urban dust and rural surface soil samples.

	Background value*	BJC (n = 30)				MYT (n = 10)				MYC(n = 36)				Sediment (n = 1)	Recovery rate**	
		Mean	Min	Max	SD	Mean	Min	Max	SD	Mean	min	Max	SD		min	Max
As (μg/g)	9.7	4.34	2.85	6.83	0.77	5.62	3.32	8.37	1.51	6.61	1.81	18.38	3.03	3.10	0.867	1.12
Ba (μg/g)	531	728	596	932	95	754	595	1100	163	631	500	1119	109	886	0.958	1.05
Cd (μg/g)	0.074	0.48	0.18	1.37	0.22	0.90	0.34	3.16	0.85	0.27	0.08	1.00	0.19	0.22	0.832	1.22
Ce (μg/g)	77.3	57.9	45.5	71.6	6.4	63.4	54.6	70.4	4.7	76.3	48.6	139.6	17.1	83.4	0.971	1.14
Co (μg/g)	15.6	8.9	6.0	21.9	2.6	12.3	9.6	17.6	2.4	14.4	8.1	24.1	4.2	10.2	0.923	1.07
Cr (μg/g)	68.1	109.3	49.6	233.0	38.2	114.3	65.0	217.8	41.9	89.4	48.0	215.5	38.9	59.6	0.827	1.16
Cu (μg/g)	23.6	102.5	29.0	475.1	94.0	62.3	36.3	118.3	26.8	34.9	18.1	64.0	12.0	31.5	0.925	1.04
Hg (μg/g)	0.069	0.33	0.04	3.69	0.67	0.81	0.07	6.16	1.88	0.08	0.02	0.63	0.10	0.08	0.823	1.10
La (μg/g)	42.7	28.3	21.6	33.2	3.0	32.5	27.4	36.2	2.7	38.0	24.2	75.3	9.3	45.8	0.914	1.09
Mn (μg/g)	705	524	393	713	62	685	513	1000	162	725	337	1314	174	610	0.951	1.06
Mo (μg/g)	4.1	2.26	0.89	5.85	1.27	1.78	1.06	4.39	1.00	0.84	0.44	2.54	0.41	0.65	0.803	1.12
Nb (μg/g)	10	11.0	8.8	13.2	1.1	11.6	8.5	13.4	1.5	13.3	5.0	27.7	3.8	10.0	0.862	1.10
Nd (μg/g)	39.9	23.0	17.3	29.1	2.4	29.4	25.3	47.3	6.5	35.2	22.1	58.3	7.3	32.4	0.952	1.08
Ni (μg/g)	29	25.9	14.5	60.3	7.7	30.4	20.5	52.2	9.3	34.9	17.0	76.5	12.1	32.0	0.949	1.12
Pb (μg/g)	25.4	68.8	35.0	134.3	22.0	85.3	46.4	221.2	57.9	30.9	11.7	164.5	24.0	23.8	0.966	1.12
Rb (μg/g)	99	56.2	31.2	68.3	7.8	66.8	55.7	85.2	9.5	74.0	19.4	101.0	15.2	49.6	0.836	1.07
Sb (μg/g)	1.1	6.07	1.63	26.33	5.20	2.72	1.46	7.63	1.82	0.75	0.27	1.65	0.22	0.34	0.934	1.22
Sc (μg/g)	11.44	8.2	7.0	9.7	0.6	10.4	9.2	13.1	1.1	11.8	8.2	18.3	2.4	8.2	0.863	1.16
Sr (μg/g)	202	323	249	366	32	349	310	386	24	232	143	406	66	435	0.909	1.07
Ti (μg/g)	4300	3601	3035	4906	411	3713	3386	4111	237	4376	2016	11,067	1434	2679	0.881	1.11
Tl (μg/g)	0.461	0.43	0.33	0.57	0.05	0.58	0.34	1.02	0.24	0.48	0.27	0.74	0.13	0.21	0.859	1.11
Y (μg/g)	24.8	20.6	16.2	23.9	1.8	23.6	19.9	27.6	2.4	25.6	9.6	32.7	4.3	18.8	0.971	1.18
Zn (μg/g)	102.6	264	123	444	88	318	175	977	240	98	64	168	27	92	0.942	1.07
Al (%)	6.99	5.43	4.97	6.03	0.24	5.10	4.36	5.89	0.46	6.46	5.11	8.04	0.75	5.47	0.856	1.17
Fe (%)	2.97	2.87	1.96	4.05	0.44	4.54	3.23	9.49	1.90	4.04	2.60	7.20	1.06	2.81	0.972	1.06
Mg (%)	1.27	1.90	0.89	3.27	0.45	1.83	1.03	2.57	0.43	1.27	0.47	2.26	0.44	1.20	0.956	1.07
Ca (%)	1.52	5.26	2.76	7.75	0.94	4.75	2.97	5.96	1.03	1.85	0.32	4.84	0.92	11.35	0.925	1.04
Na (%)	1.31	1.58	1.22	1.75	0.14	1.96	1.39	3.19	0.63	1.55	0.18	2.65	0.35	1.77	0.949	1.04
K (%)	1.93	1.67	1.39	1.86	0.12	1.60	1.20	2.09	0.24	1.97	1.47	3.06	0.29	1.84	0.945	1.02

Note: *The background value of Beijing region (reference: China National Environmental Monitoring Center, 1990) **Recovery rate has no unit.

corresponding mean values, which are shaded in Table 1. The SD values of the other metals are all less than half of the corresponding mean values. Results showed that these metals have relatively different contents at different locations and thus might have different emission sources. Human activities should be the major source of these metals, except Mo, which has a content of below the background value in most samples.

Ratios between individual element contents and the background values were calculated for each sample and the mean and maximum values are shown in Fig. 2. There are few anthropogenic emissions and accumulations for As, Ce, Co, La, Mn, Mo, Nd, Ni, Rb, Sc, Ti, Tl, Y, Al, and K in the study area with ratios close to or less than 1. Clearly identifiable human activity emissions and influences were demonstrated by larger ratios ranging from 1 to 2 for Ba, Cr, Nb, Sr, Fe, Mg and Na and higher than 2 for Cd, Cu, Hg, Pb, Sb, Zn, and Ca. The contents of Ba, Cd, Cr, Cu, Hg, Pb, Sb, Sr, Zn, Ca and Mg in urban dust from BJC and MYT were higher than those from MYC and higher than the background values (Fig. 2), which suggests that the emissions of these elements are mainly caused by human activities in cities. Overall, Cd, Cu, Hg, Pb, Sb, and Zn demonstrated to be the typical urban contaminants and mostly influenced by the adjacent human activities with higher content to background ratios and SD values. Ca also had higher content to background ratios whereas smaller SD values, showing that it was mainly from urban anthropogenic emissions and relatively evenly distributed in the study areas.

For the sediment sample, the contents of Ba, Cd, Ce, Cu, Hg, La, Ni, Sr, Ca, and Na were higher than the Beijing background values.

3.2. Spatial distribution of metals

Eight metals (Ba, Cd, Cu, Hg, Pb, Sb, Zn, and Ca), which exhibited

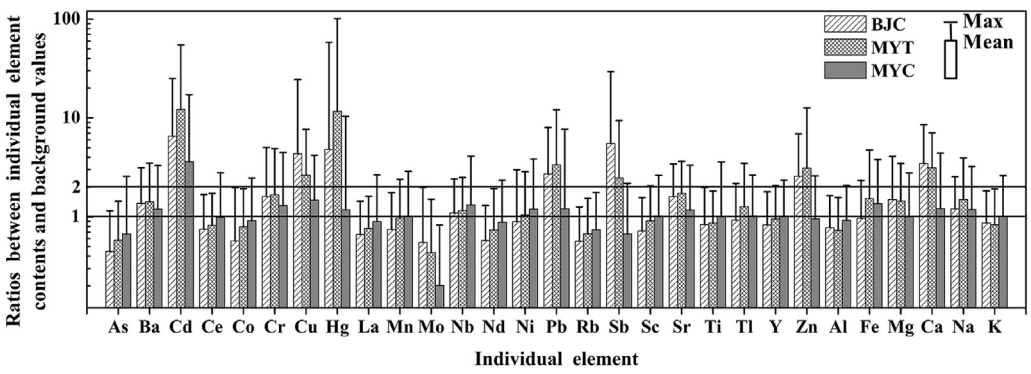

Fig. 2. Ratios between individual element contents and background values.

Please cite this article in press as: Yu, Y., et al., Metal enrichment and lead isotope analysis for source apportionment in the urban dust and rural surface soil, Environmental Pollution (2016), http://dx.doi.org/10.1016/j.envpol.2016.06.046

much higher metal contents than the background values at certain sites, were selected to demonstrate their spatial distribution in the three sampling areas using the IDW in ArcGIS 10.0 (Fig. 3). The background levels of individual metals are all within the first content ranges in Fig. 3 with dark green color.

The enrichment levels of all eight metals in BJC and MYT were higher than found in MYC, showing that there were intensive anthropogenic emissions from cities. Table 2 shows the important anthropogenic pollution sources for certain metal elements from previous studies. The X in the table represents the potential source is an important emission source for the corresponding metal element.

Fig. 3 showed the metal contents were quite different at different locations and varied very much for different metal elements, which exhibited quite diverse shapes and colors in Fig. 3. This is caused by the abundant impact from adjacent anthropogenic pollution emissions at various locations and different emission sources for different metal elements. Among the plotted eight metal elements, Cu and Sb demonstrated much higher contents in urban dust of BJC than those of MYT. Little enrichment of Cu and Sb was found in MYC. This showed that the emission sources of Cu and Sb mainly existed in cities. Among the 29 metal elements investigated, Cu and Sb were found to be the most distinct elements that were highly affected by the developing level and congestion status of the cities with much higher contents in dust in more developed and congested cities, e.g. BJC. The higher contents of Cu and Sb in BJC might be mainly due to the heavy traffic and increased brake usage in congested super city based on the fact that brake system was the main emission source of Cu and Sb shown in Table 2. In addition, higher Cu and Sb contents happened in southern and western part of BJC, where many long distance bus stations and railway stations located. This is another evidence that vehicle braking system emits much Cu and Sb.

In MYT, the highest contents of nearly all the eight metals except Hg occurred around MYT5, the central area of MYT. As a small scale town with about 19,000 capita (http://www.my.bjstats.gov.cn/Page/181/InfoID/11739/SourceId/717/PubDate/2011-05-06/default.aspx), MYT5 was surrounded by the most important buildings of the town within 500 m radius range including Miyun county government center, Miyun county hospital, Miyun grand theater, Scitech outlet plaza (Miyun), Changan Shopping center. Therefore adjacent anthropogenic activity intensity largely determined the environmental metal contents and Ba, Cd, Cu, Pb, Sb, Zn, and Ca were found to be good indicators.

3.3. Pb isotope characteristics and Pb potential sources

To further understand the origin of Pb in the urban dust and surface soil, the Pb isotopic ratios (e.g., $^{204}Pb/^{206}Pb$, $^{207}Pb/^{206}Pb$, and $^{208}Pb/^{206}Pb$) of three study areas and the major possible sources, such as vehicle exhaust, industries, and coal, were shown in Fig. 4. The Pb isotope ratios for Cenozoic basalts and Mesozoic–Cenozoic granites in Hebei Province were used as the background value (Zhang, 1989; Basu et al., 1991; Zhu, 1995). The Chinese coal line was the distribution of $^{208}Pb/^{206}Pb$ and $^{207}Pb/^{206}Pb$ of coal and coal combustion emissions from different areas and different thermal power stations in China (Mukai et al., 2001; Gao et al., 2004; Chen et al., 2005; Tan et al., 2006; Hu et al., 2013). It demonstrated the Pb isotope characters of major coals in China–ranges and relationship between $^{208}Pb/^{206}Pb$ and $^{207}Pb/^{206}Pb$. The Chinese coal line showed a similar Pb ratio to the Chinese Pb ore line, which was obtained from the data of Zheng et al. (2004) and Zhu et al. (2013). Results suggested that the coal and Pb ore have similar Pb isotope ratios, which were both underground resources. The Chinese coal and Pb ores were generally higher in $^{208}Pb/^{206}Pb$ ratio (Cumming and Richards, 1975; Hu et al., 2015a) than the Pb growth curve (Fig. 4). Fig. 4 showed that the Pb isotope ratio $^{204}Pb/^{206}Pb$ and $^{207}Pb/^{206}Pb$ increase in the following sequence: loess < vehicle exhaust < industry < aerosols. Coal combustion had a wider Pb ratio range, which covered the variability from vehicle exhaust and industrial processes.

For the samples collected in this study, the Pb isotope ratios of MYC soil covered the widest ratio ranges with $^{204}Pb/^{206}Pb$, $^{207}Pb/^{206}Pb$, and $^{208}Pb/^{206}Pb$ of 0.0544–0.0635, 0.8496–0.9560, and 2.0790–2.3201, respectively, demonstrating a wide range of Pb sources in the MYC surface soil. Site MYC5, located in an iron mine, had the highest $^{204}Pb/^{206}Pb$, $^{207}Pb/^{206}Pb$, and $^{208}Pb/^{206}Pb$ ratios in all samples, which indicated that the ore had higher $^{204}Pb/^{206}Pb$, $^{207}Pb/^{206}Pb$, and $^{208}Pb/^{206}Pb$ ratios than other sources.

The Pb isotope ratios of urban dust in BJC and MYT, except BJC29 and MYT6, remained within a relatively narrow range, which indicated relatively consistent sources for urban dust. The three Pb isotope ratios for urban dust in BJC were distributed similarly to the MYT dust. The $^{208}Pb/^{206}Pb$ values of BJC and MYT all located below the Chinese coal line and Chinese Pb ore line, whereas the values of MYC were almost on these lines. Therefore Pb pollution in MYC was mainly related to the coal combustion. Most samples located higher than the Pb growth curve, except MYC33, showing that anthropogenic influences are present in the study area. The ratio of sediment sample was higher than most samples, indicating different Pb sources.

As shown in Fig. 4, the fine particle subsamples, BJC14b and BJC28b, had higher $^{204}Pb/^{206}Pb$, $^{207}Pb/^{206}Pb$, and $^{208}Pb/^{206}Pb$ ratios than the coarse particle subsamples. The fine particle subsamples were located near the anthropogenic sources of coal combustion and vehicle exhaust, and the coarse particle subsamples were located near the background value. This indicated that fine particle subsamples might be more related to surrounding human activities than coarse subsamples.

The $^{204}Pb/^{206}Pb$ and $^{208}Pb/^{206}Pb$ ratios of the aerosols in Beijing (Liu et al., 2011) were generally higher than the urban dust samples (Fig. 4). Atmospheric deposition has an important influence on urban dust and rural surface soil, and the particles can transfer between aerosols and urban dust, rural surface soil (Bi et al., 2007). In this situation, atmospheric deposition can bring anthropogenic pollution from other areas for urban dust and rural surface soil. But the pollution from atmospheric deposition is the secondary pollution and is the combination of many end-members or different sources. Therefore, atmospheric deposition cannot be thought of as the original sources of urban dust and rural surface soil.

3.4. Source identification based on Pb isotope ratios

The Pb isotope ratios from various sources were used to quantify the Pb pollution contribution proportion from different sources. As shown in the previous discussion, coal combustion, vehicle exhaust, and industrial activities had a major influence on Pb pollution in the study area. Therefore, four end-members (e.g., background, coal combustion, vehicle exhaust, and industry) were assumed to contribute 100% to the Pb in the samples. If the proportions of each of the end-members k were known, the Pb isotope ratios can be calculated as follows:

$$(207/206)_{c,i} = \sum_{j=1}^{4} k_{j,i}(207/206)_j \quad (1)$$

Please cite this article in press as: Yu, Y., et al., Metal enrichment and lead isotope analysis for source apportionment in the urban dust and rural surface soil, Environmental Pollution (2016), http://dx.doi.org/10.1016/j.envpol.2016.06.046

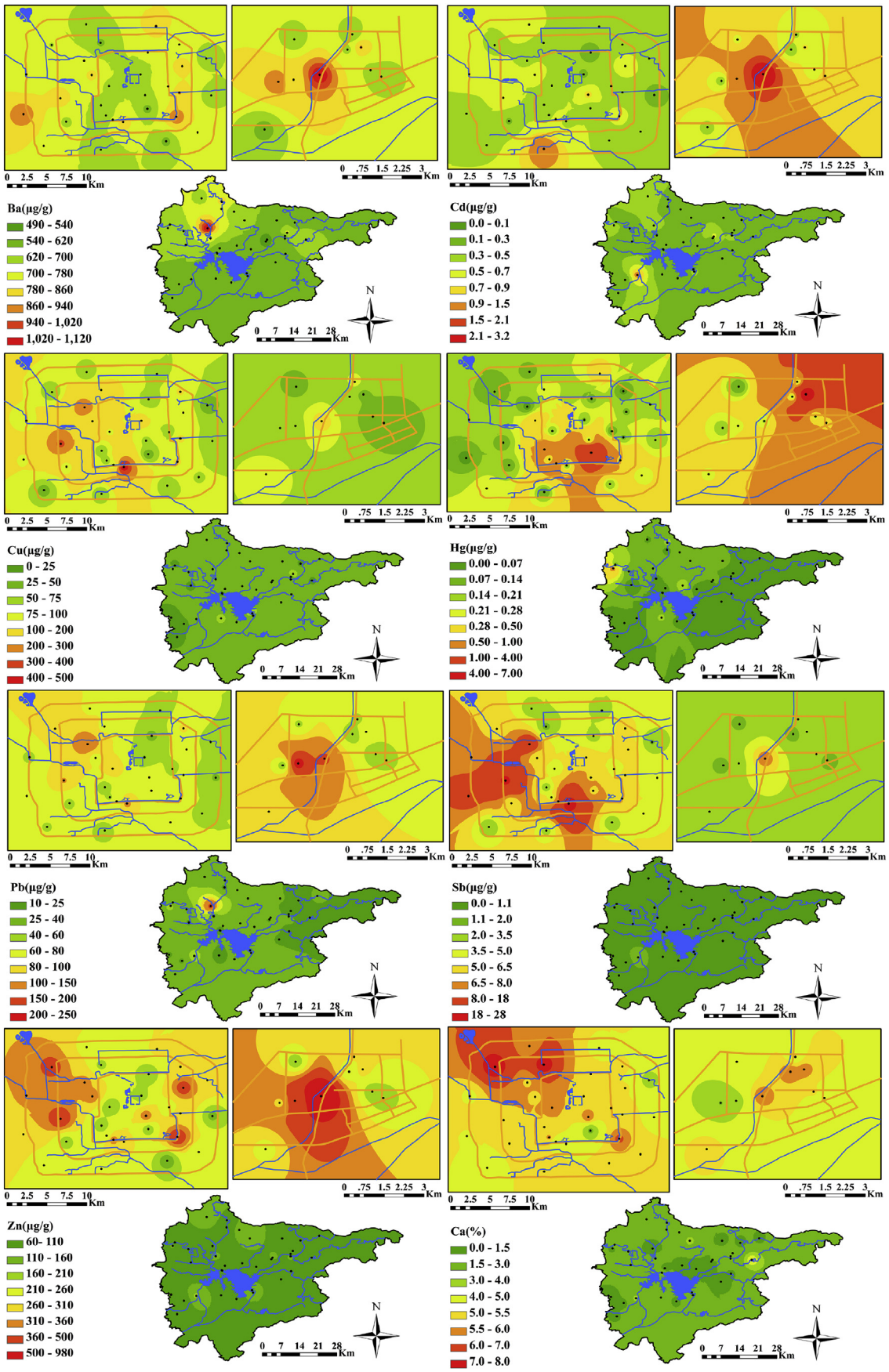

Fig. 3. Spatial distribution of selected metals in urban dust and rural surface soils.

Please cite this article in press as: Yu, Y., et al., Metal enrichment and lead isotope analysis for source apportionment in the urban dust and rural surface soil, Environmental Pollution (2016), http://dx.doi.org/10.1016/j.envpol.2016.06.046

Table 2
Potential sources of metals from different industries and vehicles.

Potential sources	Ba	Cd	Cr	Cu	Pb	Sb	Sr	Zn	Al	Fe	Ca	Hg	Mg
Braking system	×	–	–	×	–	×	–	–	–	×	–	–	–
Automobile metal part wear	–	–	×	–	–	–	–	–	×	×	–	–	×
Tire tread wear	–	–	–	–	–	–	–	×	×	–	×	–	–
Paints on road	×	–	×	–	×	–	–	–	–	–	×	–	–
Vehicle exhaust	×	–	–	×	×	–	–	×	–	–	×	–	–
Cement	–	–	–	–	–	–	×	–	×	×	×	–	–
Building weathering	–	×	–	–	×	–	–	×	–	–	–	–	–
Coal consumption	–	–	×	×	×	–	×	–	–	–	–	–	–
Iron mine	–	×	–	×	–	–	–	–	–	×	–	–	–
Pesticides and fertilizers	–	×	–	×	×	–	–	×	–	×	×	×	–

*References: Li et al., 2001; Adachi and Tainosho, 2004; Widory et al., 2010; Charlesworth et al., 2011.

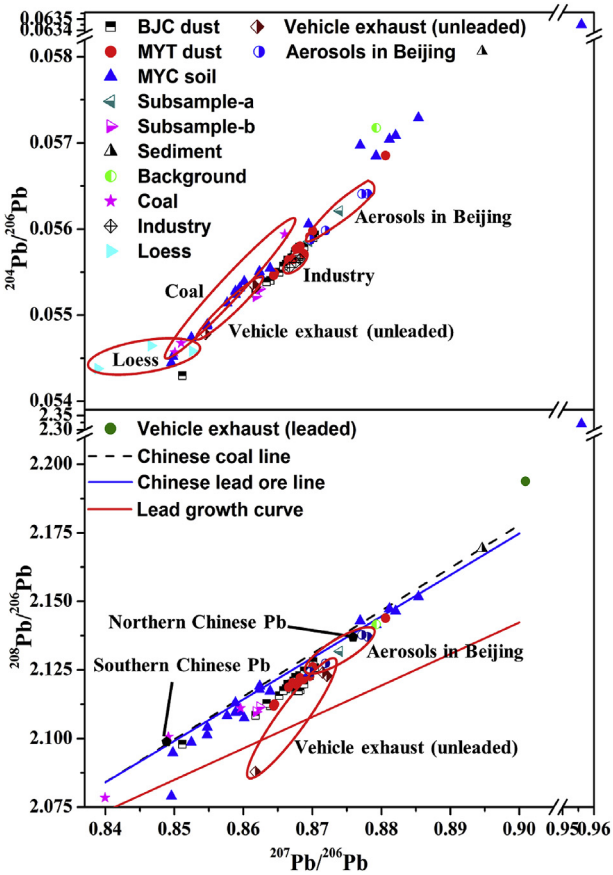

Fig. 4. Pb isotopic composition for urban dust and rural surface soil samples and some possible sources, $^{204}Pb/^{206}Pb$ vs $^{207}Pb/^{206}Pb$ and $^{208}Pb/^{206}Pb$ vs $^{207}Pb/^{206}Pb$.
Data Sources: Background - from Zhang (1989), Basu et al. (1991) and Zhu (1995), Aerosols in Beijing- mainly from Liu et al. (2011), Coal - including coal combustion, from Mukai et al. (2001); Gao et al. (2004); Tan et al. (2006); Widory et al. (2010), Industry - mainly from lead refining plants near Beijing, Widory et al. (2010), Vehicle exhaust - including gasoline and diesel, Zhu et al. (2001), Gao et al. (2004), Chen et al. (2005), Tan et al. (2006), Loess - obtained from Widory et al. (2010), Chinese coal line - drawn based on data from Mukai et al. (2001); Gao et al. (2004); Chen et al. (2005); Tan et al. (2006); Hu et al. (2013), Chinese lead ore line - obtained from the linear regression of data from Zheng et al. (2004), Zhu et al. (2013), Lead growth curve - from Cumming and Richards (1975); Hu et al. (2015a).

$$(204/206)_{c,i} = \sum_{j=1}^{4} k_{j,i}(204/206)_j \quad (2)$$

$$(208/206)_{c,i} = \sum_{j=1}^{4} k_{j,i}(208/206)_j \quad (3)$$

$$\sum_{j=1}^{4} k_{j,i} = 1, \text{where } 0 \le k_{j,i} \le 1 \quad (4)$$

where $(207/206)_{c,i}$, $(204/206)_{c,i}$, and $(208/206)_{c,i}$ represent the calculated $^{207}Pb/^{206}Pb$, $^{204}Pb/^{206}Pb$, and $^{208}Pb/^{206}Pb$ ratios for sample I, respectively; $(207/206)_j$, $(204/206)_j$, and $(208/206)_j$ give the $^{207}Pb/^{206}Pb$, $^{204}Pb/^{206}Pb$, and $^{208}Pb/^{206}Pb$ ratios for end-member j, respectively; j represents the end-members with $j = 1$ for background, $j = 2$ for coal combustion, $j = 3$ for vehicle exhaust, and $j = 4$ for industry; and $k_{j,i}$ is the mass proportion of end-member j for sample i. The Pb isotope ratios for the end-members were achieved from related studies and the mean values of different studies were calculated as shown in Table 3. Only the Pb isotope ratios of the end-members background, coal combustion, and industrial activities from Beijing area were used to calculate the pollution source proportion. For vehicle exhaust, the data from other cities were also used due to the unified standard for gasoline and diesel in the whole China.

To obtain Pb isotope ratio proportions for different end-members, a least-square optimization method was used to minimize the sum of squared differences between the calculated and observed isotope ratios with the objective function as follows:

$$F(k_{j,i}) = \min \sum \left(\left((207/206)_{c,i} - (207/206)_i \right)^2 + \left((204/206)_{c,i} - (204/206)_i \right)^2 + \left((208/206)_{c,i} - (208/206)_i \right)^2 \right) \quad (5)$$

where $(207/206)_{c,i}$, $(204/206)_{c,i}$, and $(208/206)_{c,i}$ are described as Equations (1)–(4) and $(207/206)_i$, $(204/206)_i$, and $(208/206)_i$ are the observed isotope ratios for sample i.

Lsqlin in Matlab R2010b was used to obtain the optimized solution. The mass proportions of different end-members for each sample $k_{j,i}$were calculated and results were shown in Fig. 5. Coal and vehicle exhaust were the most important Pb pollution sources and the average of the sum of their mean mass fraction was 74.6% of the total Pb pollution. The calculated mass proportions of different pollution sources had a large variance for MYC samples but a much smaller variance for BJC and MYT samples, indicating relatively similar Pb pollution compositions for different locations in the urban area. The Pb pollution proportion from industry was the lowest in the urban area with mean fractions of 9.7% and 11.5% for BJC and

Please cite this article in press as: Yu, Y., et al., Metal enrichment and lead isotope analysis for source apportionment in the urban dust and rural surface soil, Environmental Pollution (2016), http://dx.doi.org/10.1016/j.envpol.2016.06.046

Table 3
Lead isotope ratios of four end-members.

	$(207/206)_j$	$(204/206)_j$	$(208/206)_j$	References
Background (j = 1)	0.9060	0.0591	2.1416	Zhang, 1989; Basu et al., 1991; Zhu, 1995
Coal (j = 2)	0.8551	0.0552	2.1007	Mukai et al., 2001; Widory et al., 2010
Vehicle exhaust (j = 3)	0.8643	0.0552	2.1116	Zhu et al., 2001; Gao et al., 2004; Chen et al., 2005; Tan et al., 2006
Industry (j = 4)	0.8748	0.0562	2.1961	Zhu et al., 2003; Widory et al., 2010

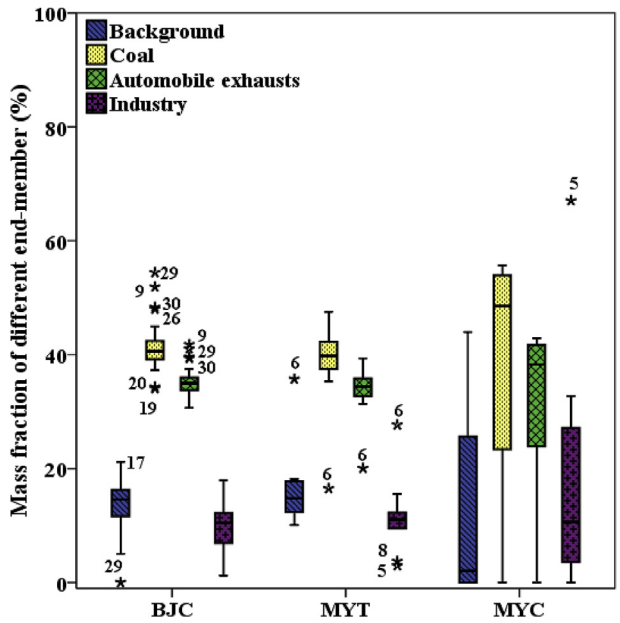

Fig. 5. Mass proportion of different pollution sources in BJC, MYT, and MYC through the Pb isotope ratio calculations.

MYT, respectively. Coal combustion had the highest Pb pollution fraction with mean values of 41.5%, 38.6%, and 39.8% for BJC, MYT, and MYC, respectively. This result indicated that Pb pollution from coal combustion was the major source of Pb pollution in study area. This was coincident with coal was still the major energy source for China (Xie et al., 2015). The large variance of calculated Pb mass proportions for MYC indicated a much more uncertainty of Pb sources apportionment for MYC soil than for the urban dust. Previous studies also showed a variety of anthropogenic Pb input into surface soils including traffic activities, industries, and so on (Facchinelli et al., 2001; Wong et al., 2002; Micó et al., 2006).

Vehicle exhaust was the second most important Pb pollution source with mean fractions of 35.3%, 33.6%, and 33.0% for BJC, MYT, and MYC, respectively. Although leaded gasoline was banned in 1997 in Beijing (Hu et al., 2015b), the results demonstrated major Pb pollution from vehicle exhaust, which may be from diesel and low-quality unleaded gasoline fuels.

For subsamples BJC14b and BJC28b, the Pb pollution from coal and vehicle exhaust was stronger than from the corresponding coarse particles. The mass fractions from the background in BJC14a and BJC28a were higher than those in BJC14b and BJC28b. This confirms that there was more anthropogenic Pb pollution in the fine particles than in the corresponding coarse particles (Lau and Stenstrom, 2005).

The Pb pollution mass fractions for the sediment samples were 52.5% from background, 0.0185% from coal, 6.2% from vehicle exhaust, and 41.5% from industry. This result suggests that the Pb pollution in sediment was mainly from the background soil and upstream industry discharges. More attention should be paid to the industrial wastewater discharge into the river for better pollution control.

4. Conclusions

The influence of human activities on metal contents in urban surface dust and rural surface soils was well demonstrated by the large metal content to background values. Among the 29 metals studied, the ratio of observed to background was higher than 2 for Cd, Cu, Hg, Pb, Sb, Zn, and Ca. The contents of Ba, Cd, Cr, Cu, Hg, Pb, Sb, Sr, Zn, Ca and Mg from the urban areas of BJC and MYT were higher than those from rural MYC, suggesting that the elevated contents were mainly caused by the increased human activities in the urban areas. Spatial distribution showed that Cu and Sb contents were the most distinctive metal elements mainly influenced by different development and congestion levels.

The Pb isotope ratios (e.g., $^{204}Pb/^{206}Pb$, $^{207}Pb/^{206}Pb$, and $^{208}Pb/^{206}Pb$) were used to understand the origin of Pb sources in further detail. The Pb isotope ratios of urban dust from BJC and MYT had a narrower range than MYC, and located near the Pb isotope ratios of anthropogenic inputs. Most of the samples had a lower $^{208}Pb/^{206}Pb$ ratio than the Chinese coal line and Chinese Pb ore line. Quantitative calculation results for the end-members proportion showed that coal combustion had the highest mass fraction for Pb pollution and vehicle exhaust was the second largest pollution source. In addition, urban dust with the particles smaller than 120 μm got more anthropogenic Pb influence than coarse particles.

For river sediment, the Pb isotope results showed that the Pb pollution in river sediment was mainly caused by the background and up-stream industrial sources.

Acknowledgment

This research was supported by the Fund for Innovative Research Group of the National Natural Science Foundation of China (Grant No. 51421065), National Science Foundation of China (Grant 51278054), the State Key Program of National Natural Science of China (Grant 41530635), the Fundamental Research Funds for the Central Universities, and China Scholarship Council. The authors are grateful for the support.

Appendix A. Supplementary data

Supplementary data related to this article can be found at http://dx.doi.org/10.1016/j.envpol.2016.06.046.

References

Acosta, J.A., Gabarrón, M., Faz, A., Martínez-Martínez, S., Zornoza, R., Arocena, J.M., 2015. Influence of population density on the concentration and speciation of metals in the soil and street dust from urban areas. Chemosphere 134, 328–337.
Adachi, K., Tainosho, Y., 2004. Characterization of heavy metal particles embedded in tire dust. Environ. Int. 30, 1009–1017.
Ault, W.U., Senechal, R.G., Erlebach, W.E., 1970. Isotopic composition as a natural tracer of lead in the environment. Environ. Sci. Technol. 4, 305–313.
Basu, A.R., Junwen, W., Wankang, H., Guanghong, X., Tatsumoto, M., 1991. Major element, REE, and Pb, Nd and Sr isotopic geochemistry of Cenozoic volcanic rocks of eastern China: implications for their origin from suboceanic-type

mantle reservoirs. Earth Planet. Sci. Lett. 105, 149–169.
Beijing Statistics Bureau, 2013. Beijing Statistical Yearbook. China Statistics Press, Beijing (in Chinese).
Bi, X., Feng, Y., Wu, J., Wang, Y., Zhu, T., 2007. Source apportionment of PM_{10} in six cities of northern China. Atmos. Environ. 41, 903–912.
Bi, X., Liang, S., Li, X., 2013. A novel in situ method for sampling urban soil dust: particle size distribution, trace metal concentrations, and stable lead isotopes. Environ. Pollut. 177, 48–57.
Charlesworth, S., Miguel, E., Ordóñez, A., 2011. A review of the distribution of particulate trace elements in urban terrestrial environments and its application to considerations of risk. Environ. Geochem. Health 33, 103–123.
Chen, J., Tan, M., Li, Y., Zhang, Y., Lu, W., Tong, Y., Zhang, G., Li, Y., 2005. A lead isotope record of Shanghai atmospheric lead emissions in total suspended particles during the period of phasing out of leaded gasoline. Atmos. Environ. 39, 1245–1253.
Cheng, H., Hu, Y., 2010. Lead (Pb) isotopic fingerprinting and its applications in lead pollution studies in China: a review. Environ. Pollut. 158, 1134–1146.
China National Environmental Monitoring Center, 1990. The Background Concentrations of Soil Elements of China. China Environmental Science Press, Beijing (in Chinese).
Christoforidis, A., Stamatis, N., 2009. Heavy metal contamination in street dust and roadside soil along the major national road in Kavala's region, Greece. Geoderma 151, 257–263.
Cumming, G.L., Richards, J.R., 1975. Ore lead isotope ratios in a continuously changing earth. Earth Planet. Sci. Lett. 28, 155–171.
Davis, A.P., Shokouhian, M., Ni, S., 2001. Loading estimates of lead, copper, cadmium, and zinc in urban runoff from specific sources. Chemosphere 44, 997–1009.
Diaz-Somoano, M., Kylander, M.E., Lopez-Anton, M.A., Suarez-Ruiz, I., Martinez-Tarazona, M.R., Ferrat, M., Kober, B., Weiss, D.J., 2009. Stable lead isotope compositions in selected coals from around the world and implications for present day aerosol source tracing. Environ. Sci. Technol. 43, 1078–1085.
Egodawatta, P., Ziyath, A.M., Goonetilleke, A., 2013. Characterising metal build-up on urban road surfaces. Environ. Pollut. 176, 87–91.
Facchinelli, A., Sacchi, E., Mallen, L., 2001. Multivariate statistical and GIS-based approach to identify heavy metal sources in soils. Environ. Pollut. 114, 313–324.
Faure, G., 1986. Principles of Isotope Geology. John Wiley and Sons, New York.
Franco-Uría, A., López-Mateo, C., Roca, E., Fernández-Marcos, M.L., 2009. Source identification of heavy metals in pastureland by multivariate analysis in NW Spain. J. Hazard. Mater. 165, 1008–1015.
Gao, Z., Yin, G., Ni, S., Zhang, C., 2004. Geochemical features of the urban environmental lead isotope in Chengdu city. Carsologica Sin. 23, 267–272 (in Chinese).
Gao, B., Zhou, H., Liang, X., Tu, X., 2013. Cd isotopes as a potential source tracer of metal pollution in river sediments. Environ. Pollut. 181, 340–343.
GB, 1995. Soil Environmental Quality Standard (GB15618-1995) (in Chinese).
Granero, S., Domingo, J.L., 2002. Levels of metals in soils of Alcalá de Henares, Spain: human health risks. Environ. Int. 28, 159–164.
Gu, Y., Wang, Z., Lu, S., Jiang, S., Mu, D., Shu, Y., 2012. Multivariate statistical and GIS-based approach to identify source of anthropogenic impacts on metallic elements in sediments from the mid Guangdong coasts, China. Environ. Pollut. 163, 248–255.
Han, L., Gao, B., Wei, X., Gao, L., Xu, D., Sun, K., 2015. The characteristic of Pb isotopic compositions in different chemical fractions in sediments from Three Gorges Reservoir, China. Environ. Pollut. 206, 627–635 (in Chinese).
http://www.my.bjstats.gov.cn/Page/181/InfoID/11739/SourceId/717/PubDate/2011-05-06/default.aspx
Hu, G., Yu, R., Zheng, Z., 2013. Application of stable lead isotopes in tracing heavy-metal pollution sources in the sediments. Acta Sci. Circumstantiae 33, 1326–1331 (in Chinese).
Hu, X., Sun, Y., Ding, Z., Zhang, Y., Wu, J., Lian, H., Wang, T., 2014. Lead contamination and transfer in urban environmental compartments analyzed by lead levels and isotopic compositions. Environ. Pollut. 187, 42–48.
Hu, N., Huang, P., Liu, J., Shi, X., Ma, D., Zhu, A., Zhang, J., Zhang, H., He, L., 2015a. Tracking lead origin in the Yellow River Estuary and nearby Bohai Sea based on its isotopic composition. Estuarine. Coast. Shelf Sci. 163, 99–107.
Hu, N., Huang, P., Zhang, H., Zhu, A., He, L., Zhang, J., Liu, J., Shi, X., Ma, D., 2015b. Tracing the Pb origin using stable Pb isotope ratios in sediments of Liaodong Bay, China. Cont. Shelf Res. 111, 268–278.
Ip, C.C.M., Li, X.D., Zhang, G., Wong, C.S.C., Zhang, W.L., 2005. Heavy metal and Pb isotopic compositions of aquatic organisms in the Pearl River Estuary, South China. Environ. Pollut. 138, 494–504.
Lau, S., Stenstrom, M.K., 2005. Metals and PAHs adsorbed to street particles. Water Res. 39, 4083–4092.
Lau, S., Han, Y., Kang, J., Kayhanian, M., Stenstrom, M.K., 2009. Characteristics of highway stormwater runoff in Los Angeles: metals and polycyclic aromatic hydrocarbons. Water Environ. Res. 81, 308–318.
Li, X., Poon, C., Liu, P.S., 2001. Heavy metal contamination of urban soils and street dusts in Hong Kong. Appl. Geochem. 16, 1361–1368.
Li, Y., Xiang, L., Tian, P., Liu, J., 2013. Desorption characteristics of total phosphorus and heavy metals from impervious urban surface sediments. Chin. Sci. Bull. 58, 3357–3360.
Li, Y., Yu, Y., Yang, Z., Shen, Z., Wang, X., Cai, Y., 2016. A comparison of metal distribution in surface dust and soil among super city, town, and rural area. Environ. Sci. Pollut. Res. 23, 7849–7860.
Liu, X., Zhu, X., Dong, S., Li, Y., Widory, D., Yang, H., Li, B., 2011. Lead isotopic measurements and source study for size-selective aerosol samples in Beijing. J. Chin. Mass Spectrom. Soc. 32 (in Chinese).
Liu, E., Yan, T., Birch, G., Zhu, Y., 2014. Pollution and health risk of potentially toxic metals in urban road dust in Nanjing, a mega-city of China. Sci. Total Environ. 476–477, 522–531.
Lu, X., Wang, L., Li, L.Y., Lei, K., Huang, L., Kang, D., 2010. Multivariate statistical analysis of heavy metals in street dust of Baoji, NW China. J. Hazard. Mater. 173, 744–749.
Lu, X., Zhang, X., Li, L.Y., Chen, H., 2014. Assessment of metals pollution and health risk in dust from nursery schools in Xi'an, China. Environ. Res. 128, 27–34.
Madarang, K.J., Kang, J., 2014. Evaluation of accuracy of linear regression models in predicting urban stormwater discharge characteristics. J. Environ. Sci. 26, 1313–1320.
Micó, C., Recatalá, L., Peris, M., Sánchez, J., 2006. Assessing heavy metal sources in agricultural soils of an European Mediterranean area by multivariate analysis. Chemosphere 65, 863–872.
Mukai, H., Tanaka, A., Fujii, T., Zeng, Y., Hong, Y., Tang, J., Guo, S., Xue, H., Sun, Z., Zhou, J., Xue, D., Zhao, J., Zhai, G., Gu, J., Zhai, P., 2001. Regional characteristics of sulfur and lead isotope ratios in the atmosphere at several chinese urban sites. Environ. Sci. Technol. 35, 1064–1071.
Sezgin, N., Ozcan, H.K., Demir, G., Nemlioglu, S., Bayat, C., 2004. Determination of heavy metal concentrations in street dusts in Istanbul E-5 highway. Environ. Int. 29, 979–985.
Song, N., Ma, J., Yu, Y., Yang, Z., Li, Y., 2015. New observations on PAH pollution in old heavy industry cities in northeastern China. Environ. Pollut. 205, 415–423.
Stigliani, W.M., Doelman, P., Salomons, W., Schulin, R., Smidt, G.R., Van der Zee, S.E.A.T., 1991. Chemical time bombs: predicting the unpredictable. Environ. Sci. Policy Sustain. Dev. 33, 4–30.
Tan, M.G., Zhang, G.L., Li, X.L., Zhang, Y.X., Yue, W.S., Chen, J.M., Wang, Y.S., Li, A.G., Li, Y., Zhang, Y.M., Shan, Z.C., 2006. Comprehensive study of lead pollution in shanghai by multiple techniques. Anal. Chem. 78, 8044–8050.
Widory, D., Liu, X., Dong, S., 2010. Isotopes as tracers of sources of lead and strontium in aerosols (TSP & PM2.5) in Beijing. Atmos. Environ. 44, 3679–3687.
Wong, S.C., Li, X.D., Zhang, G., Qi, S.H., Min, Y.S., 2002. Heavy metals in agricultural soils of the pearl river delta, South China. Environ. Pollut. 119, 33–44.
Xie, W., Sheng, P., Guo, X., 2015. Coal, oil, or clean energy: which contributes most to the low energy efficiency in China? Util. Policy 35, 67–71.
Zhang, L., 1989. Petrogenetic and Minerogenetic Theories and Prospecting, 267. Press of Beijing Technological University, Beijing (in Chinese).
Zhao, H., Li, X., 2013. Risk assessment of metals in road-deposited sediment along an urban–rural gradient. Environ. Pollut. 174, 297–304.
Zheng, J., Tan, M., Shibata, Y., Tanaka, A., Li, Y., Zhang, G., Zhang, Y., Shan, Z., 2004. Characteristics of lead isotope ratios and elemental concentrations in PM_{10} fraction of airborne particulate matter in Shanghai after the phase-out of leaded gasoline. Atmos. Environ. 38, 1191–1200.
Zhu, B., 1995. The mapping of geochemical provinces in China based on Pb isotopes. J. Geochem. Explor. 55, 171–181.
Zhu, B., Chen, Y., Peng, J., 2001. Lead isotope geochemistry of the urban environment in the Pearl River Delta. Appl. Geochem. 16, 409–417.
Zhu, B., Chen, Y., Chang, X., 2003. Application of Pb isotopic mapping to environment evaluation in China. Chem. Speciat. Bioavailab. 14, 49–56.
Zhu, Z., Sun, G., Bi, X., Li, Z., Yu, G., 2013. Identification of trace metal pollution in urban dust from kindergartens using magnetic, geochemical and lead isotopic analyses. Atmos. Environ. 77, 9–15.
Žibret, G., 2012. Impact of dust filter installation in ironworks and construction on brownfield area on the toxic metal concentration in street and house dust (Celje, Slovenia). Ambio 41, 292–301.

Please cite this article in press as: Yu, Y., et al., Metal enrichment and lead isotope analysis for source apportionment in the urban dust and rural surface soil, Environmental Pollution (2016), http://dx.doi.org/10.1016/j.envpol.2016.06.046